Supporting Information for:

# Improving Fatigue Resistance of Dihydropyrene by Encapsulation within a Coordination Cage

Martina Canton,[a,b,†] Angela B. Grommet,[a,†] Luca Pesce,[c] Julius Gemen,[a] Shiming Li,[d] Yael Diskin-Posner,[e] Alberto Credi,[b] Giovanni M. Pavan,[c,f] Joakim Andréasson,[d] Rafal Klajn*[,a]

[a]Department of Organic Chemistry, Weizmann Institute of Science, Rehovot 76100, Israel

[b]Center for Light-Activated Nanostructures (CLAN) and Dipartimento di Chimica Industriale, Università di Bologna, 40136 Bologna, Italy

[c]Department of Innovative Technologies, University of Applied Sciences and Arts of Southern Switzerland, Galleria 2, Via Cantonale 2C, CH_6928 Manno, Switzerland

[d]Department of Chemistry and Chemical Engineering, Chalmers University of Technology, 41296 Göteborg, Sweden

[e]Chemical Research Support, Weizmann Institute of Science, Rehovot 76100, Israel

[f]Department of Applied Science and Technology, Politecnico di Torino, Corso Duca degli Abruzzi 24, 10129 Torino, Italy

[†]These authors contributed equally.

## Table of contents

## 1. General information

Reagents and solvents were purchased and used as supplied unless otherwise noted. 1,3,5-Tris(1-imidazolyl)-benzene, cage **1**, and DHP were prepared according to modified literature procedures. For the characterization of 1,3,5-tris(1-imidazolyl)benzene, cage **1**, and DHP, $^1$H NMR spectra were recorded on a 300 MHz spectrometer (Bruker Avance III-300), a 500 MHz spectrometer (Bruker Avance III HD-500), and a 400 MHz spectrometer (Agilent 400), respectively. For the characterization of inclusion complexes, $^1$H NMR spectra were recorded on a 400 MHz spectrometer (Bruker Avance III-400) and $^1$H DOSY, $^1$H–$^1$H COSY, and $^1$H–$^1$H NOESY spectra were recorded on a 500 MHz spectrometer (Bruker Avance III HD 500). Unless stated otherwise, all NMR experiments were performed at a constant temperature of 298 K. $^1$H chemical shifts ($\delta_H$) are expressed in parts-per-million (ppm) and reported relative to residual solvent resonances (1.94 ppm for $CD_3CN$, 2.51 ppm for $(CD_3)_2SO$, 4.79 ppm for $D_2O$, and 7.26 ppm for $CDCl_3$). $^1$H DOSY NMR spectra were collected using temperature and gradient settings that were calibrated prior to the measurements. The diffusion coefficient of the solvent was used as a calibration standard. High-resolution mass spectrum (HRMS) of DHP was obtained using an Agilent 1290 Infinity LC system tandem to an Agilent 6520 Accurate Mass Q-TOF LC/MS with an APCI source in a positive mode. Thin-layer chromatography to monitor the reactions was performed on silica gel plates (Merck Kieselgel 60, $F_{254}$). The spots were visible under UV light. Column chromatography was performed with silica gel (Merck silica 60). UV/vis absorption spectra were recorded with a Shimadzu UV-2700 UV/vis spectrophotometer using quartz cuvettes with 1 cm pathway. Fluorescence spectra were recorded on a Cary Eclipse fluorescence spectrophotometer. For photoirradiation experiments, a Prizmatix Mic-LED 460 nm (~1.0 mW·cm$^{-2}$ at the sample) light-emitting diode (LED) was used as a blue light source, and a UVGL-25 Compact UV Lamp (~0.7 mW·cm$^{-2}$ at the sample) by UVP (4-Watt) as a UV light source.

## 2. Synthesis and characterization of triimidazole ligand

The triimidazole ligand was synthesised by modifying a procedure previously described in the literature.[1] Imidazole (2.72 g, 34.0 mmol), 1,3,5-tribromobenzene (1.26 g, 4.00 mmol), potassium carbonate (2.21 g, 15.99 mmol), and copper(II) sulfate (0.025 g, 0.16 mmol) were combined. Imidazole functions both as a reagent and as the solvent for this reaction. The flask was purged with nitrogen and heated at 180 °C. While heating, the flask was left submerged up to the neck in oil to prevent the solidification of imidazole. After 20 h, the flask was cooled to room temperature and the reaction mixture was washed thoroughly with water. The resulting solid was taken up into methanol (100 mL) and the solution was filtered to remove a dark-brown residue. The white product was precipitated out of methanol upon the addition of water and dried in a desiccator. Yield: 0.78 g (71%).

$^1$H NMR (300 MHz, DMSO-$d_6$): δ = 8.76 (s, 3H, $H_1$), 8.25 (s, 3H, $H_3$), 8.18 (s, 3H, $H_2$), 7.40 (s, 3H, $H_4$).

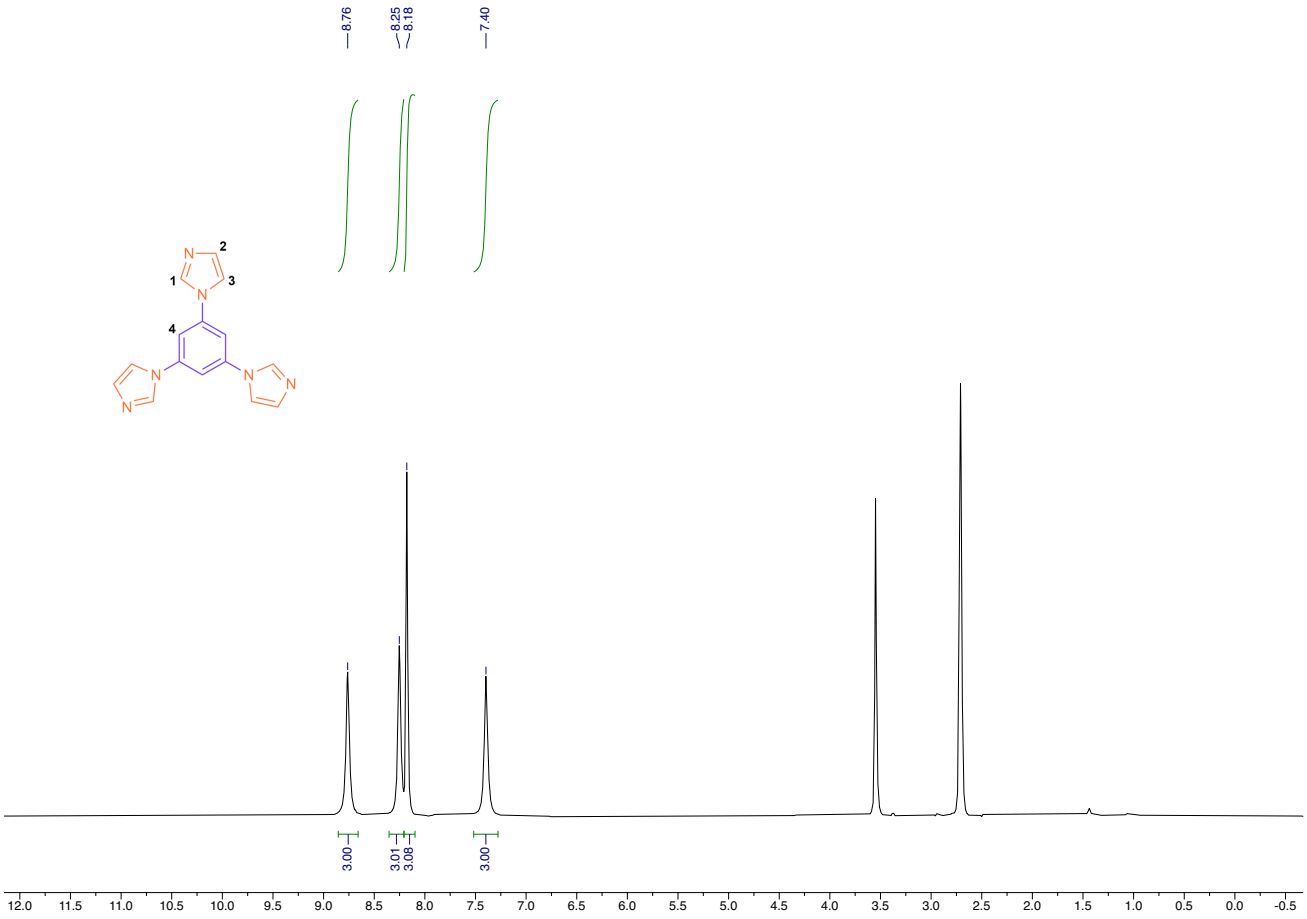


**Figure S1.** $^1$H NMR spectrum (300 MHz, DMSO-$d_6$) of 1,3,5-tris(1-imidazolyl)benzene.

## 3. Synthesis and characterization of cage **1**

Cage **1** was synthesized by modifying a procedure previously described in the literature.[2] *N*,*N*,*N*′,*N*′-tetramethylethylenediamine (TMEDA) (50 mg, 0.43 mmol) was dissolved in DMSO (6 mL) and $Pd(NO_3)_2 \cdot xH_2O$ (100 mg, 0.43 mmol) was added to the solution. The mixture was heated at 80 °C until $Pd(NO_3)_2$ dissolved (~10 min). Next, 1,3,5-tris(1-imidazolyl)benzene (74.2 mg, 0.27 mmol) was added, and the mixture was heated for an additional 2 hours. The solution was then filtered through cotton wool to remove a dark suspension, and ethyl acetate (25 mL) was added to the filtrate. The resulting precipitate was centrifuged, washed 4–5 times with anhydrous acetone, and dried under vacuum. Cage **1** was obtained as a white powder in a near-quantitative yield.

$^1$H NMR (500 MHz, $D_2O$): δ = 9.11 (s, 8H, $H_6$), 8.81 (s, 4H, $H_1$), 7.75 (s, 4H, $H_5$), 7.71 (s, 4H, $H_3$), 7.69 (s, 8H, $H_4$), 7.64 (s, 8H, $H_7$), 7.54 (s, 12H, $H_2$/$H_8$), 3.15 (s, 24H, TMEDA-$CH_2$), 2.77-2.70 (m, 72H, TMEDA-$CH_3$).

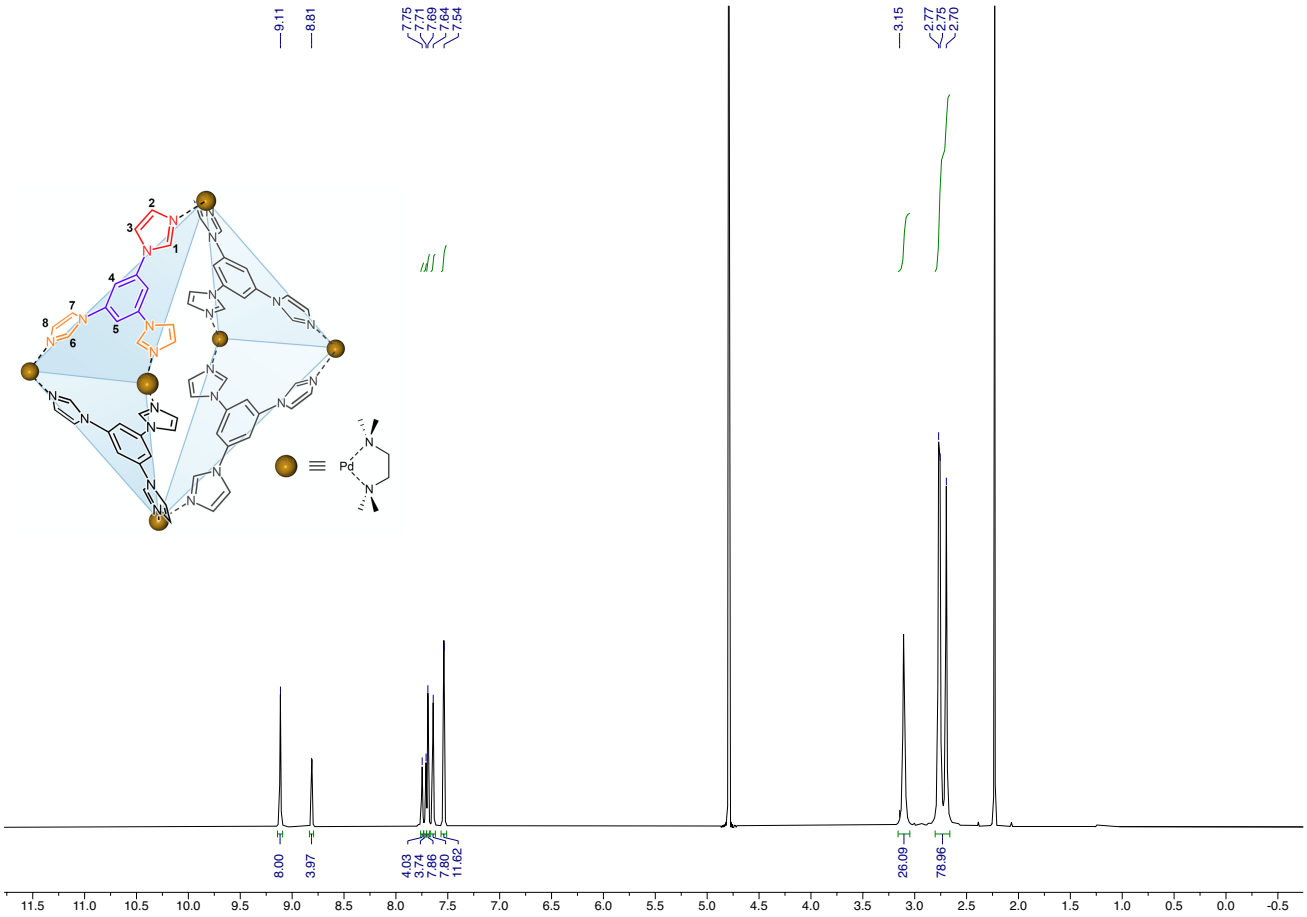


**Figure S2.** $^1$H NMR spectrum (500 MHz, $D_2O$) of cage **1**.

## 4. Synthesis and characterization of DHP

**General methods and materials for synthesis:** The reactions were monitored by thin-layer chromatography performed on silica gel plates (Merck Kieselgel 60, $F_{254}$). The spots were visible under UV light. Column chromatography was performed with silica gel (Merck silica 60). For characterization methods, see Section 1.

**Synthesis of *trans*-15,16-dimethyldihydropyrene (DHP):**

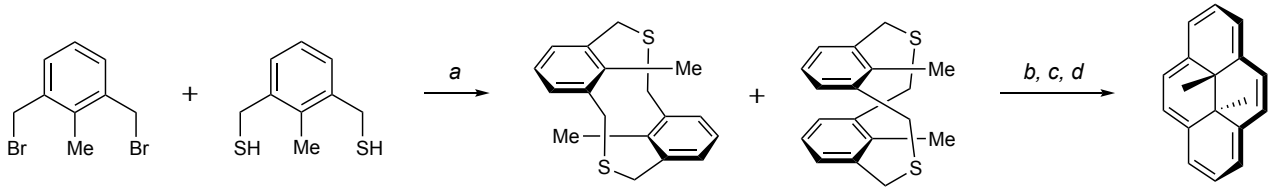


**Scheme 1.** Synthetic procedures (reagents and conditions): (*a*) Coupling reaction (NaOH, EtOH, $C_6H_6$, 80 °C, argon); (*b*) Wittig rearrangement of thiacyclophane isomers (*n*-BuLi/THF, $CH_3I$, 0 °C); (*c*) Methylation of the Wittig isomers (Borch reagent, $(CH_3O)_2CH–BF_4$, DCM, –30 °C to 20 °C); (*d*) Hofmann elimination to DHP (*t*-BuOK, THF, rt, argon).

DHP was synthesized based on previously reported literature procedures[3,4] and it was purified by flash column chromatography.

The $^1$H NMR (and $^{13}$C; not shown) data of 2,6-bis(bromomethyl)toluene,[5] 2,6-bis(mercaptomethyl)toluene,[3] *syn*-thiacyclophane,[3] *anti*-thiacyclophane,[3] and DHP[6] are consistent with those previously reported in the literature.

**2,6-Bis(bromomethyl)toluene**

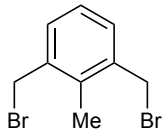


$^1$H NMR (400 MHz, $CDCl_3$): δ = 7.31 (d, *J* = 7.6 Hz, 2H, ArH), 7.15 (t, *J* = 7.6 Hz, 1H, ArH), 4.54 (s, 4H, $CH_2$), 2.44 (s, 3H, $CH_3$).

**2,6-Bis(mercaptomethyl)toluene**

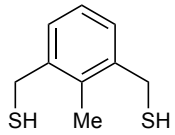


$^1$H NMR (400 MHz, $CDCl_3$): δ = 7.17–7.08 (m, 3H, ArH), 3.77 (d, *J* = 7.2 Hz, 4H, C*H*$_2$SH), 2.42 (s, 3H, $CH_3$), 1.67 (t, *J* = 7.2 Hz, 2H, $CH_2$S*H*).

***syn*-Thiacyclophane**

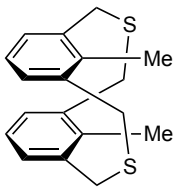


$^1$H NMR (400 MHz, $CDCl_3$): δ = 6.68-6.57 (m, 6H, ArH), 4.05-4.01 (d, *J* = 15.2 Hz, 4H, $CH_2$), 3.90-3.86 (d, *J* = 15.2 Hz, 4H, $CH_2$), 2.54 (s, 6H, $CH_3$).

**_anti_-Thiacyclophane**

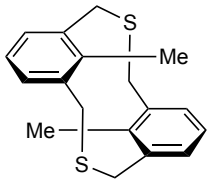


$^1$H NMR (400 MHz, $CDCl_3$): δ = 7.28 (d, *J* = 7.6, 4H, ArH), 7.09 (d, *J* = 7.6, 2H, ArH), 3.69 (s, 8H, $CH_2$), 1.29 (s, 6H, $CH_3$).

**DHP**

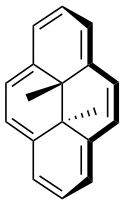

$^1$H NMR (400 MHz, $CDCl_3$): δ = 8.65 (s, 4H, ArH), 8.61 (d, *J* = 7.2 Hz, 4H, ArH), 8.14 (t, *J* = 7.6 Hz, 2H, ArH), –4.23 (s, 6H, $CH_3$).

HRMS (Q-TOF, $ESI^+$, *m*/*z*): found $[M + H]^+$ = 233.1332; calcd for $[M + H]^+$ ($C_{18}H_{16}$) = 233.1325.

**$^1$H NMR spectra:**

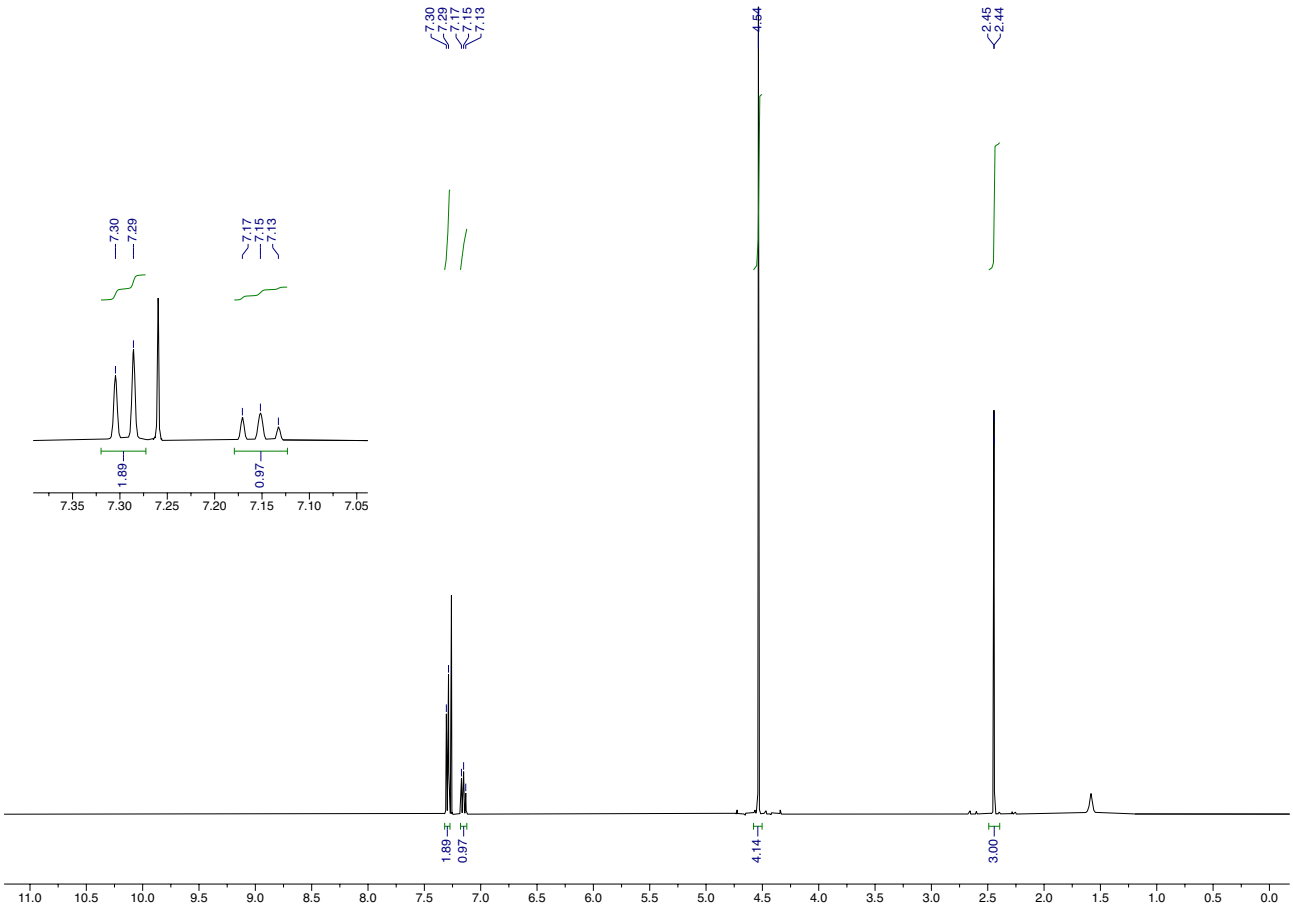


**Figure S3.** $^1$H NMR spectrum (400 MHz, $CDCl_3$) of 2,6-bis(bromomethyl)toluene.

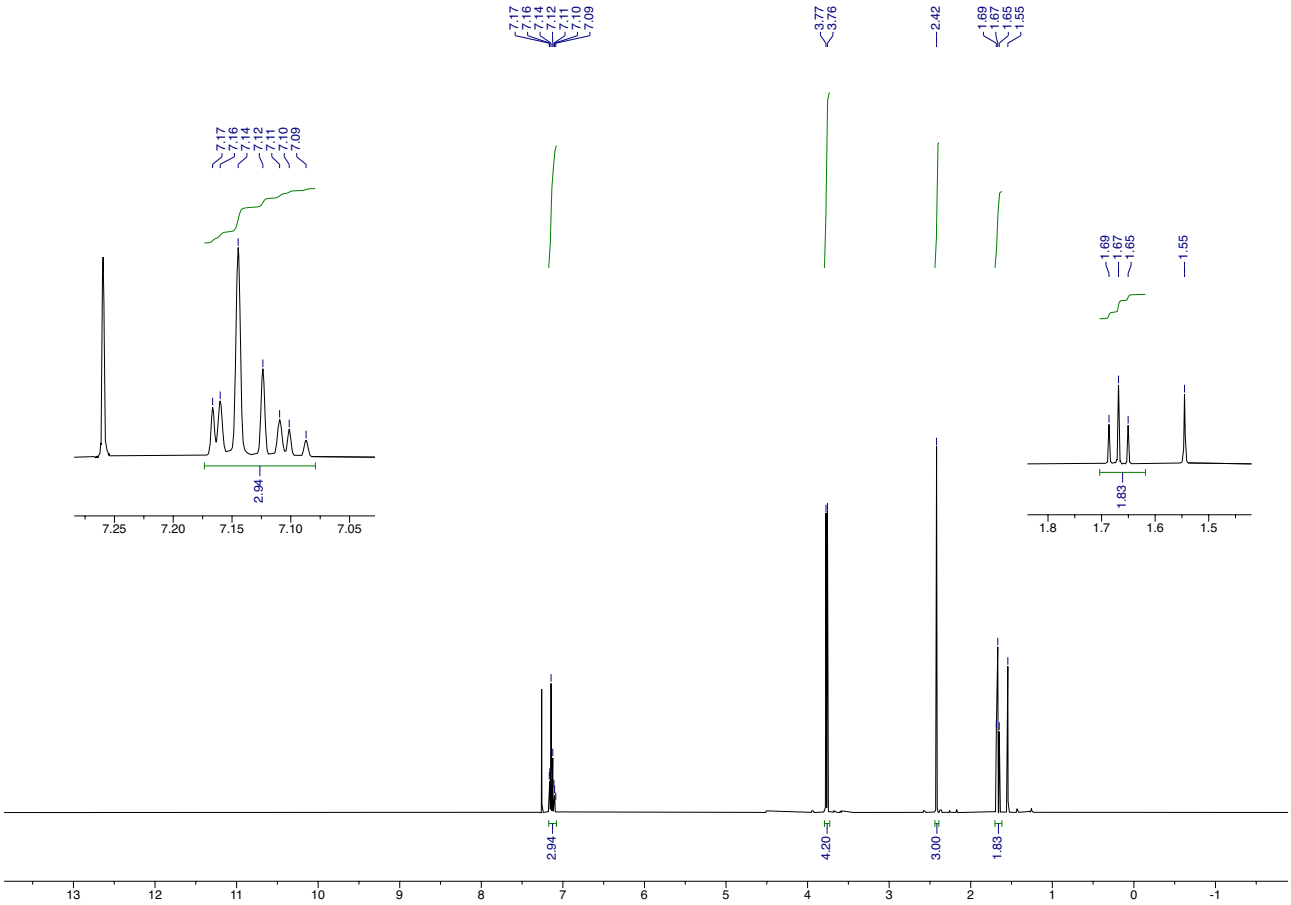


**Figure S4.** $^{1}H$ NMR spectrum (400 MHz, $CDCl_3$) of 2,6-bis(mercaptomethyl)toluene.

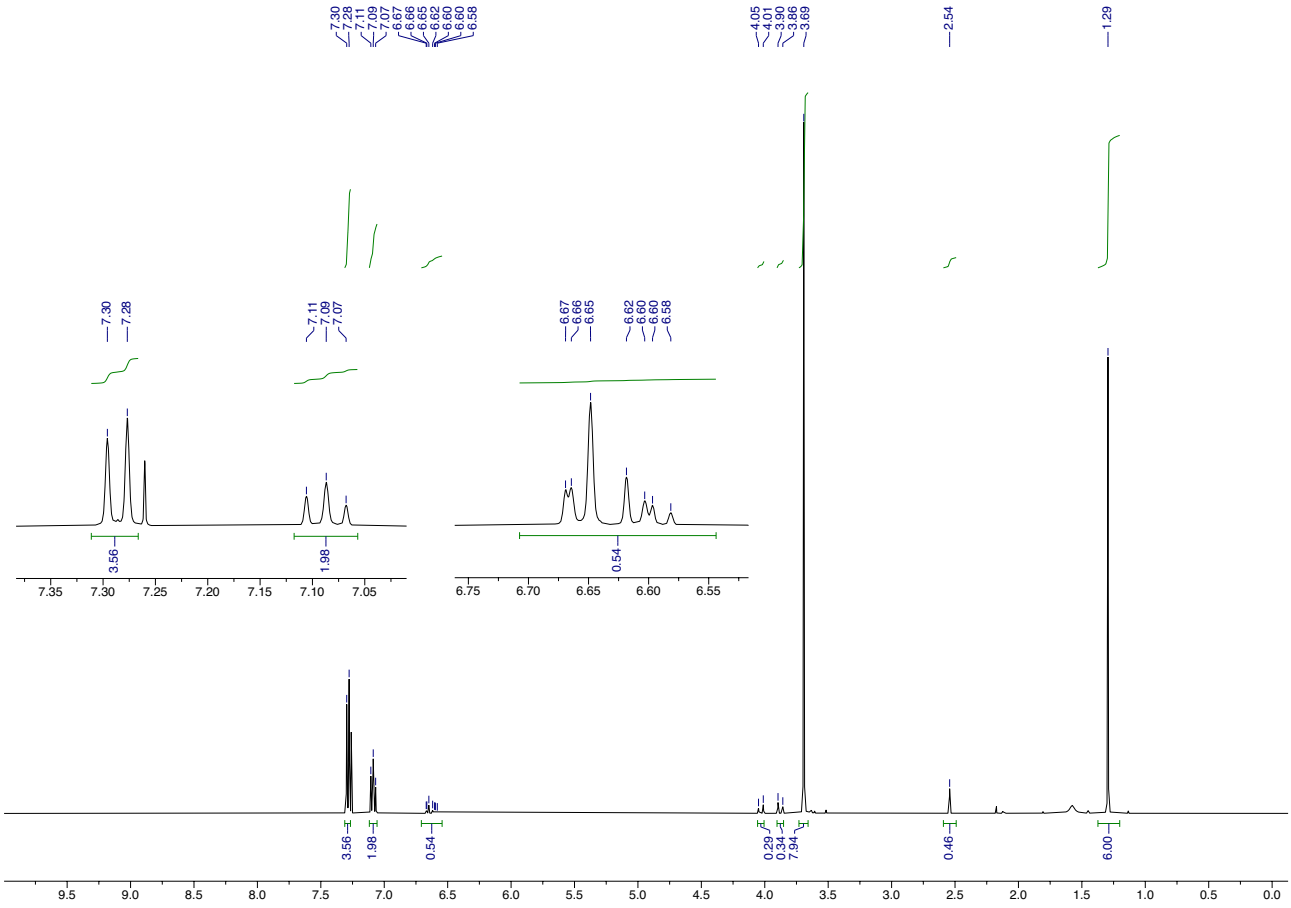

**Figure S5.** $^{1}$H NMR spectrum (400 MHz, $CDCl_3$) of a mixture of *anti*- and *syn*-thiacyclophane (*anti*/*syn* = 12:1).

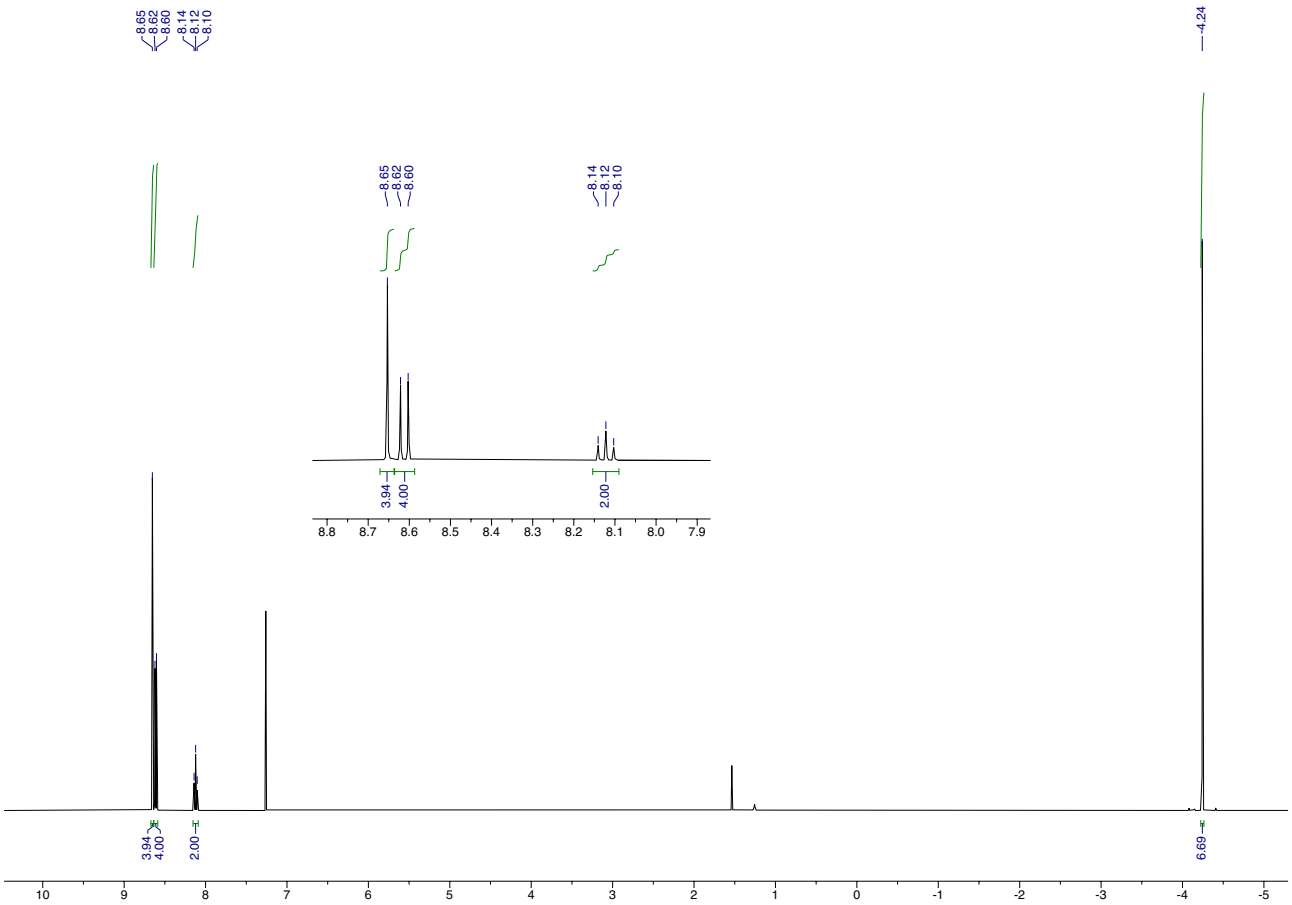


**Figure S6.** $^{1}$H NMR spectrum (400 MHz, $CDCl_3$) of *trans*-15,16-dimethyldihydropyrene (DHP).

## 5. Formation and characterization of DHP⊂**1**

Solid DHP (4.64 mg; 0.02 mmol) was added to an aqueous solution of cage **1** (6.36 mg; 0.002 mmol in 1.0 mL of $H_2O$ or $D_2O$). The mixture was stirred for 24 h at room temperature. The resulting dark green suspension was filtered through glass wool, then centrifuged at 5,000 rpm to remove solid DHP and give a transparent green solution. Encapsulation of DHP was achieved in quantitative yields, as determined by $^1$H NMR.

$^1$H NMR (400 MHz, $D_2O$): δ = 9.43 (s, 4H, $H_1$), 8.43 (s, 8H, $H_6$), 7.93 (s, 4H, $H_3$), 7.88 (s, 8H, $H_4$), 7.78 (s, 8H, $H_7$), 7.70 (s, 4H, $H_2$), 7.55 (s, 8H, $H_8$), 7.52 (d, 4H, $H_{10}$) 7.44 (s, 4H, $H_{11}$), 6.90 (t, 2H, $H_9$), 6.25 (s, 4H, $H_7$), 3.61-2.24 (m, 96H, TMEDA), –6.44 (s, 6H, $H_{12}$).

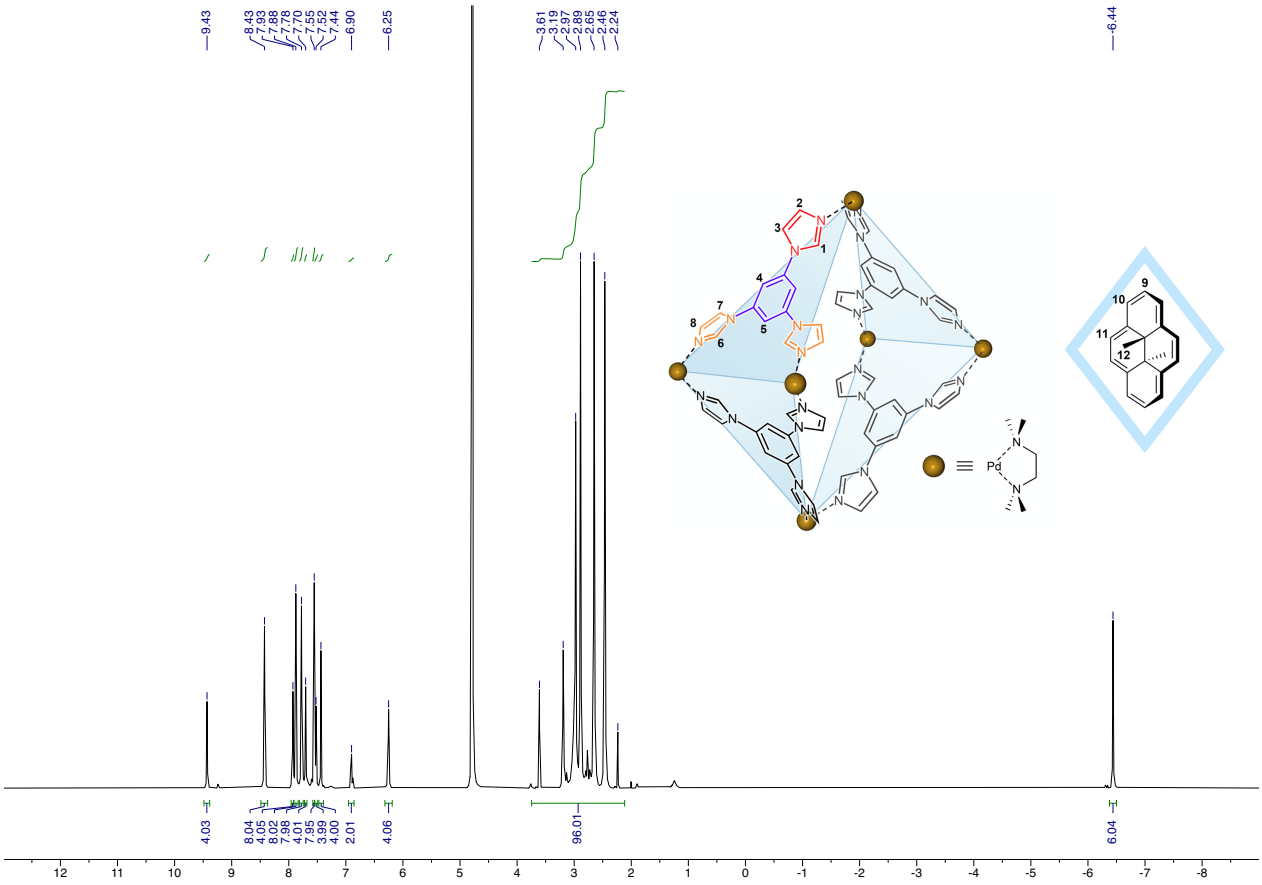


**Figure S7.** $^1$H NMR spectrum (400 MHz, $D_2O$) of DHP⊂**1**.

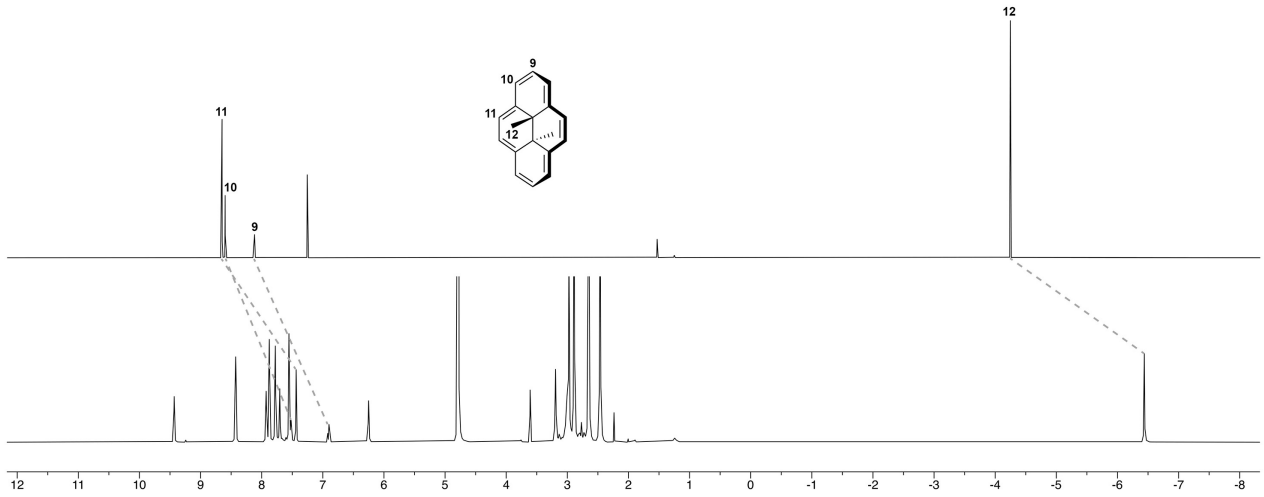


**Figure S8.** Comparison of $^{1}$H NMR spectra of free and encapsulated DHP (replotted from Figures S6 and S7, respectively).

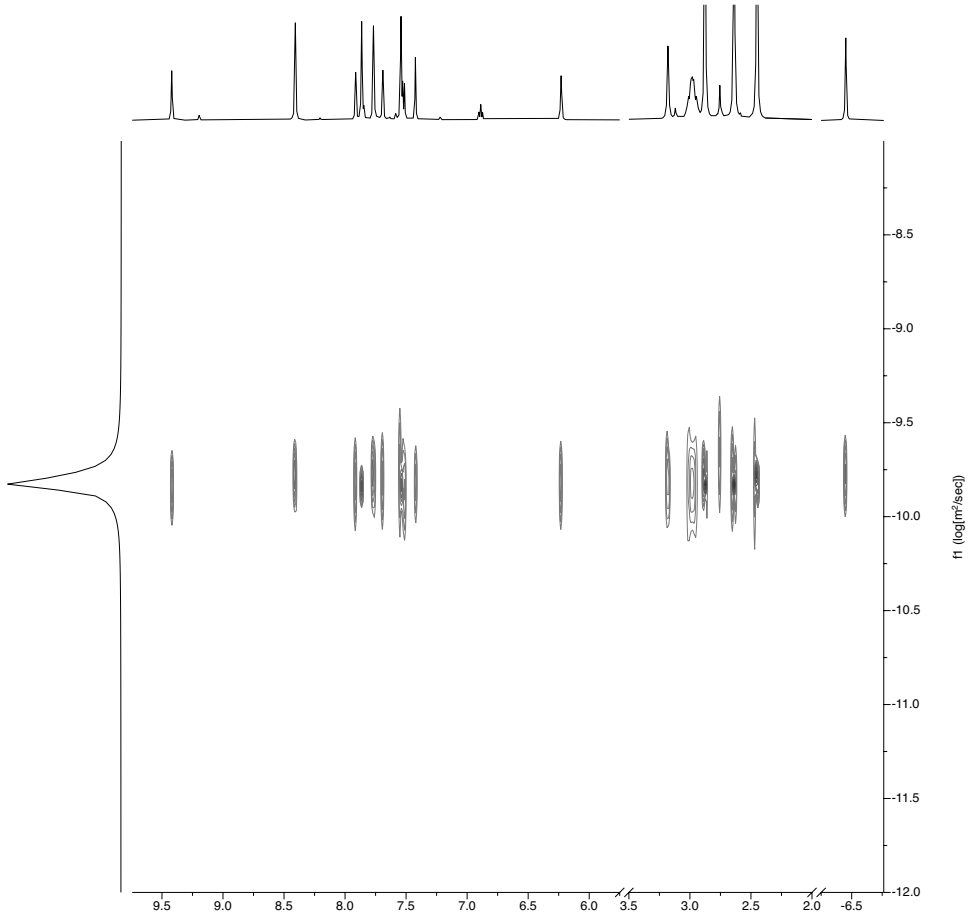


**Figure S9.** $^{1}$H DOSY NMR spectrum (500 MHz, $D_2O$) of DHP⊂**1**.

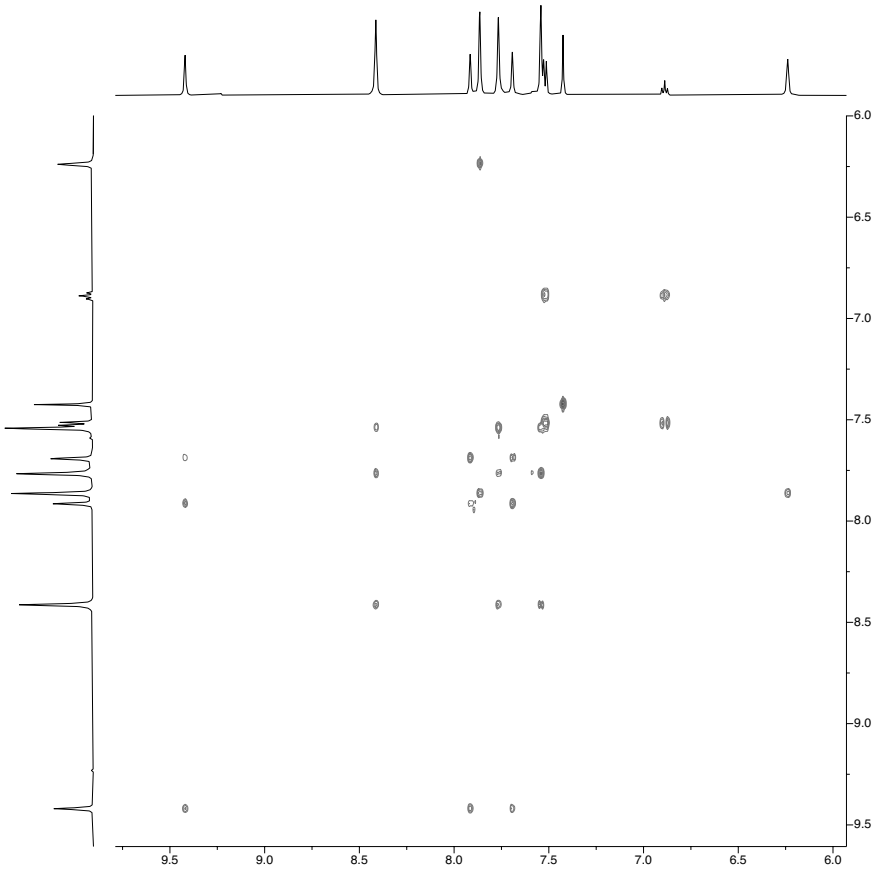


**Figure S10.** Long-range $^{1}H$–$^{1}H$ COSY NMR spectrum (500 MHz, $D_2O$) of DHP⊂**1**.

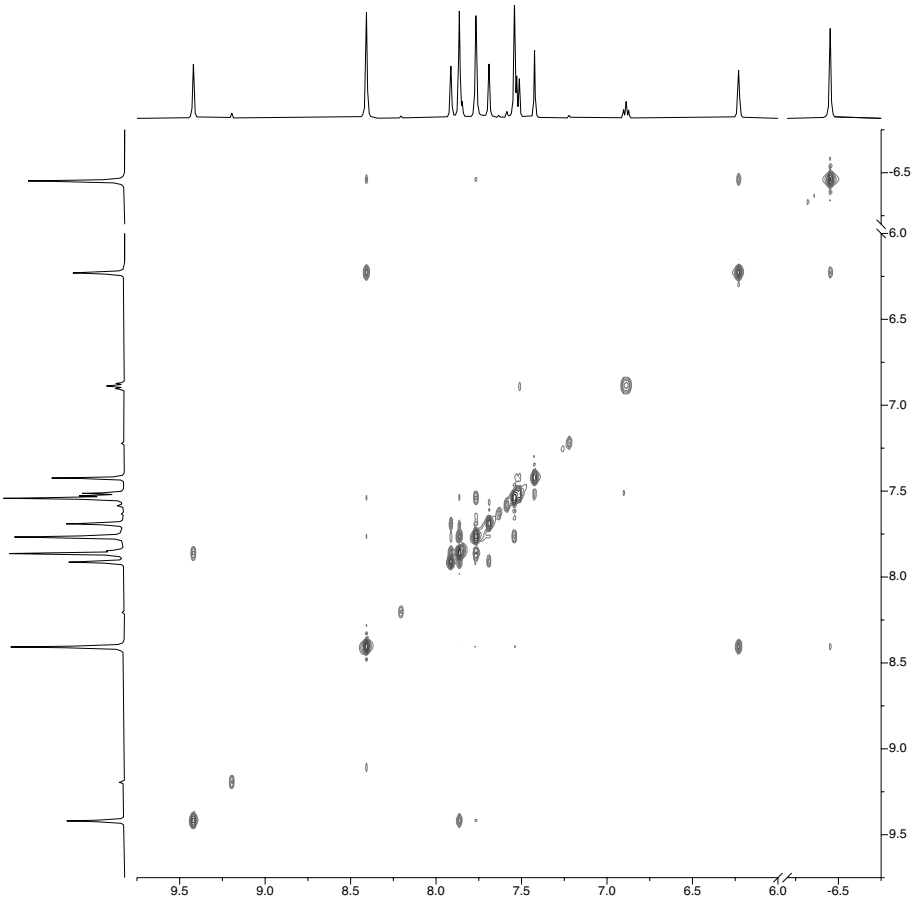


**Figure S11.** $^{1}H$–$^{1}H$ NOESY NMR spectrum (500 MHz, $D_2O$) of DHP⊂**1**.

## 6. UV/vis titration of cage **1** with DHP

To verify that the stoichiometry of the DHP–**1** inclusion complex is 1:1, we followed changes in the absorption spectra of cage **1** in water (0.62 mM, 2.0 mL) during titration with a 6.94 mM solution of DHP in MeCN. Pure **1** shows negligible absorption in the visible region (Figure S12a, bottom spectrum). Titration with DHP results in a gradual increase of the band centered at 481 nm, which is due to solubilized DHP. Solubilization of DHP cannot be explained by the presence of MeCN; in fact, we verified that DHP is insoluble even in the solvent mixture corresponding the titration end point ($H_2O$/MeCN ≈ 9:1 *v*/*v*); instead, the appearance and increase of the 481 nm band is due to encapsulation of DHP inside the cavity of **1**. Indeed, the band stopped increasing after more than 1 equiv of DHP has been added (Figure S12b). The titration can also be conveniently followed by monitoring the absorbance in the near-infrared region (e.g., at 800 nm), which is indicative of the presence of light-scattering aggregates in solution. The absorbance at 800 nm remained low until ca. 1 equiv of DHP was added. Beyond that, all the cages have been filled and the addition of subsequent aliquots of DHP results in precipitation, drastically increasing the baseline (Figure S12a and c). These results confirm that one molecule of cage **1** is capable of binding (and solubilizing in water) only one molecule of DHP.

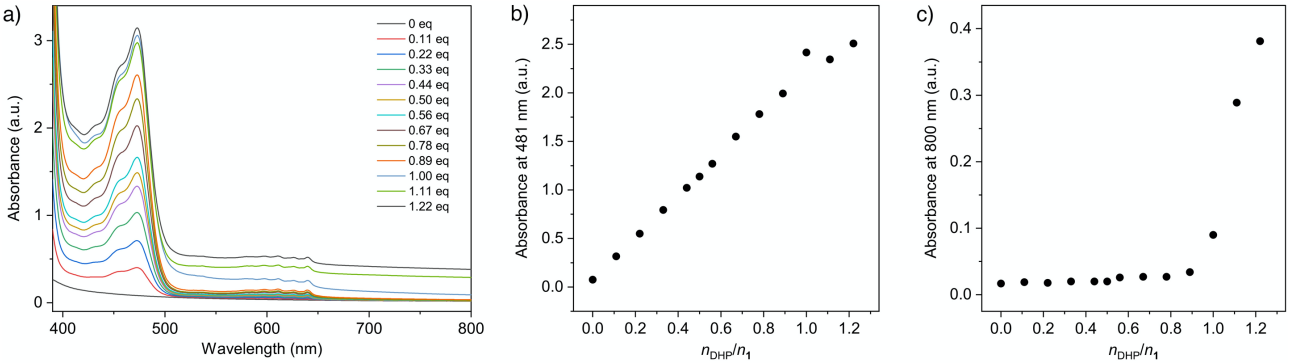


**Figure S12. a)** Absorption spectra observed upon addition of small aliquots of DHP solution (6.94 mM, MeCN) to a solution of cage **1** (0.625 mM, $H_2O$). **b)** Titration curve obtained by plotting the values of absorption due to solubilized DHP ($\lambda_{max}$ = 481 nm) as a function of the amount of DHP added. **c)** Titration curve obtained by plotting the values of absorption at 800 nm (due to aggregated DHP) as a function of the amount of DHP added.

## 7. X-ray data collection and structure refinement of DHP⊂**1**

Yellow-green prism single crystals of DHP⊂**1** were obtained by slow water evaporation from an aqueous solution of the inclusion complex. A crystal of the size 0.117 × 0.048 × 0.032 $mm^3$ was immersed in perfluorinated ether and mounted on a Mitogen LithoLoop. The crystal was flash-cooled to 100 K. Data were collected on Rigaku Xtalab PRO dual source equipped with microfocus and Dectris 200K detector.

**Crystal data:** Formula: $C_{114}H_{160}N_{48}O_{36}Pd_6$; Crystal color and shape: yellow-green prism; Crystal system: Triclinic *P-1*; Dimensions of the unit volume: a = 17.7895(3) Å, b = 20.2962(3) Å, c = 22.3737(2) Å; α = 98.7680(10)°, β = 92.1890(10)°, γ = 90.7530(10)°; Unit cell volume = 7976.53(19) $Å^3$; Temperature = 100(2) K; Z = 2; Fw = 3417.29; Calculated density = 1.423 $g·cm^{-3}$; μ = 6.038 $mm^{-1}$; Wavelength: CuKα (λ = 1.54184 Å); $-22 \le h \le 22$, $-25 \le k \le 25$, $-27 \le l \le 27$; 244232 reflections collected; 32384 independent reflections (R-int = 0.0656); Data completeness = 0.993.

The data were processed with CrysAlis$^{PRO}$ Structure was solved with SHELXT.[7] Full-matrix least-squares refinement was based on $F^2$ with SHELXL[8] and OLEX2.[9] Hydrogens were treated as isotropic in a riding mode. The water solvent molecules were removed and PLATON / SQUEEZE[10] was performed. Finally, further refinement based on $F^2$ with SHELXL on 2010 parameters with 257 restraints gave final $R_1 = 0.0670$ (based on $F^2$) with $wR_2 = 0.1679$ for data with $I > 2\sigma(I)$ and $R_1 = 0.0898$ with $wR_2 = 0.1928$ for all data on 32384 reflections, goodness-of-fit on $F^2 = 1.085$, largest electron density peak 1.934 $e·Å^{-3}$, and largest hole –1.902 $e·Å^{-3}$. Crystallographic data for the structure has been deposited with the Cambridge Crystallographic Data Centre (CCDC 1995149).

| Guest | CCDC | $d_1$ (Å) | Distortion from empty **1** (%) | Reference |
|---|---|---|---|---|
| None (empty **1**) | 1551434 | 16.865 | 0 | 11 |
| 1-Pyrenecarboxaldehyde | 867176 | 17.669 | 4.8 | 2 |
| 1-Pyrenecarboxaldehyde | 867176 | 18.147 | 7.6 | 2 |
| Sulfonated merocyanine | 1551437 | 18.292 | 8.5 | 11 |
| Phenylazotrimethylpyrazole | 1939530 | 18.374 | 8.9 | 12 |
| Azobenzene | 1551435 | 18.792 | 11.4 | 13 |
| Tetra-*o*-fluoroazobenzene | 1551438 | 18.923 | 12.2 | 13 |
| *p*-Allyloxyazobenzene | 1569281 | 19.109 | 13.3 | 13 |
| DHP | 1995149 | 19.552 | 15.9 | This work |
| DHP | 1995149 | 19.910 | 18.0 | This work |

**Table S1.** The distances between the axial palladium atoms, $d_1$, in free **1** and the inclusion complexes of **1** reported to date.

## 8. Comparison of the crystal structures of DHP⊂**1** and MC⊂**1**

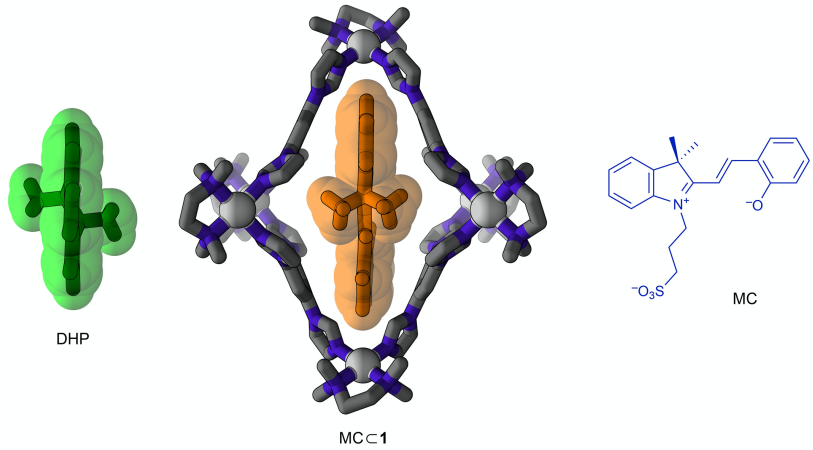


**Figure S13.** Front views of the crystal structures of DHP (left)[14] and MC encapsulated within cage **1** (MC⊂**1**; right; the $(CH_2)_3SO_3^-$ chain of MC (which protrudes out of the cage) was omitted for clarity).[11] Note that both DHP and MC are flat, except for two methyl groups protruding perpendicular to the aromatic system.

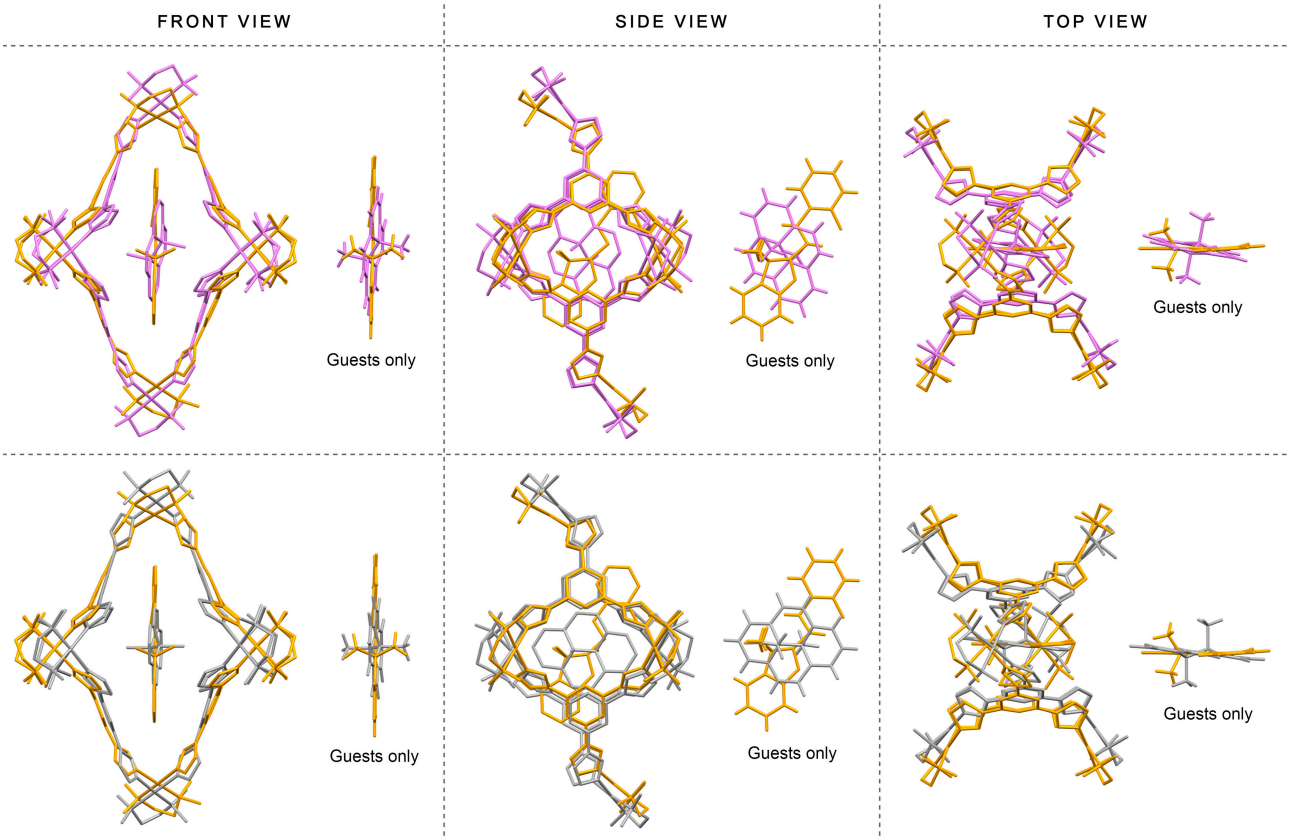


**Figure S14.** *Top:* Overlay of the crystal structures of MC⊂**1** (orange)[11] and the major conformer of DHP⊂**1** (pink). *Bottom:* Overlay of the crystal structures of MC⊂**1** (orange)[11] and the minor conformer of DHP⊂**1** (gray). We first overlaid the structures of the cages, without taking the guests into consideration. Then, the cages were removed and the resulting orientations of the guests are shown in the insets ("Guests only"). The $(CH_2)_3SO_3^-$ chain of MC (which protrudes out of the cage) was omitted for clarity. Hydrogens shown only in the insets for clarity.

## 9. Guest exchange experiments

First, DHP⊂**1** and MC⊂**1** inclusion complexes were prepared as follows. For DHP⊂**1**, cage **1** (1.00 mg, 0.31 μmol) in 1 mL of water was stirred overnight with solid DHP (0.400 mg, 1.72 μmol; >5 equiv) and excess of undissolved DHP was removed by centrifugation. 50 μL of the resulting green solution of DHP⊂**1** was diluted with 800 μL of water ($c$ = 20 μM) and absorption and fluorescence spectra (excitation wavelength = 550 nm) were recorded.

For MC⊂**1**, cage **1** (1.00 mg, 0.31 μmol) in 1 mL of water was mixed with solid MCH (0.363 mg, 0.94 μmol; 3.0 equiv) for 10 min. Note that free MCH is partially water-soluble (concentration of the saturated solution,[15] $c \approx$ 0.1 mM), therefore it was not separated from MC⊂**1** before the guest exchange experiments.

**Exchange of DHP with MC:** DHP⊂**1** (1.0 equiv) in water was added to a mixture of solid DHP (0.146 mg, 0.63 μmol; 2.0 equiv) and MCH (0.363 mg, 0.94 μmol, 3.0 equiv) and the mixture stirred vigorously. After 30 min, the mixture was centrifuged at a high speed, 50 μL of the clear supernatant was collected, diluted with 800 μL of water, and absorption and fluorescence spectra were collected. The procedure was repeated every 30 min.

**Exchange of MC with DHP:** MC⊂**1** (1.0 equiv) in water with 2.0 equiv of MCH was added to solid DHP (0.219 mg, 0.94 μmol; 3.0 equiv) and the mixture was stirred vigorously. After 30 min, the mixture was centrifuged at a high speed, 50 μL of the clear supernatant was collected, diluted with 800 μL of water, and absorption and fluorescence spectra were collected. The procedure was repeated every 30 min.

Representative UV/vis absorption spectra for both guest exchange experiments are shown in Figure 3b, c in the main text. Representative fluorescence spectra are shown in Figure S15.

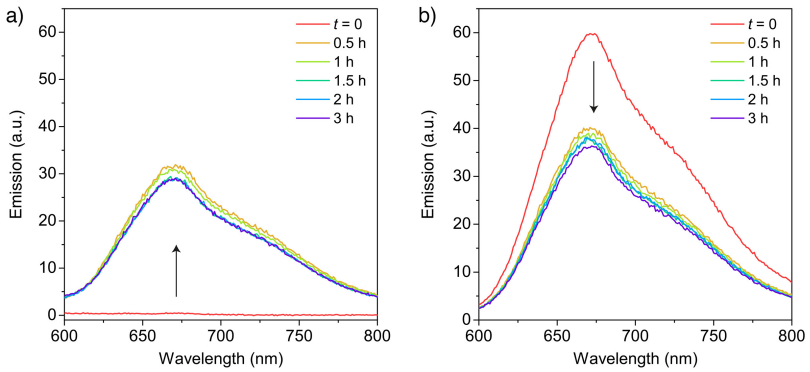


**Figure S15. a)** Evolution of fluorescence spectra upon mixing DHP⊂**1** with an equimolar amount of free MCH. **b)** Evolution of fluorescence spectra upon mixing MC⊂**1** with an equimolar amount of free DHP. Excitation wavelength, $\lambda_{exc}$ = 550 nm.

We note that although MCH is known to undergo hydrolysis in aqueous solutions,[11,16] the reaction is slow, with less than 5% decomposition within the time scale of the experiment (3 h).

## 10. Formation and characterization of CPD⊂**1**

Figure S16 shows UV/vis absorption spectra of DHP⊂**1** before (black) and after (red) exposure to 460 nm light for 10 min (after which a photostationary state (PSS) was reached), and after subsequent exposure to 254 nm light for 4 min (blue; enough to reach a PSS). The PSS under 254 nm light comprises 96% DHP⊂**1** + 4% CPD⊂**1**.

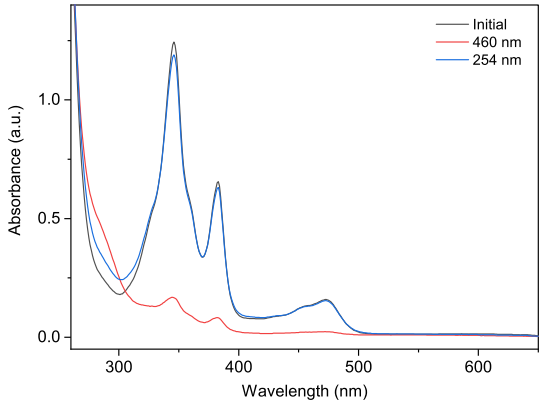


**Figure S16.** UV/vis absorption spectra of DHP⊂**1** and of the 460 nm- and 254 nm-adapted photostationary states.

To generate CPD⊂**1** at a higher concentration (here, 2 mM), a solution of DHP⊂**1** in $D_2O$ was irradiated with blue light at 460 nm for 40 min.

$^1$H NMR (500 MHz, $D_2O$): δ = 9.10 (s, 4H, $H_1$), 9.00 (s, 8H, $H_6$), 7.76 (s, 4H, $H_3$), 7.73 (s, 8H, $H_4$), 7.71 (s, 8H, $H_7$), 7.66 (s, 4H, $H_8$), 7.57 (s, 8H, $H_2$), 7.40 (d, 4H, $H_5$) 5.59 (t, 2H, $H_{13}$), 5.34 (d, 4H, $H_{14}$), 5.05 (s, 4H, $H_{15}$) 3.13-2.61 (m, 96H, TMEDA), –0.60 (s, 6H, $H_{16}$).

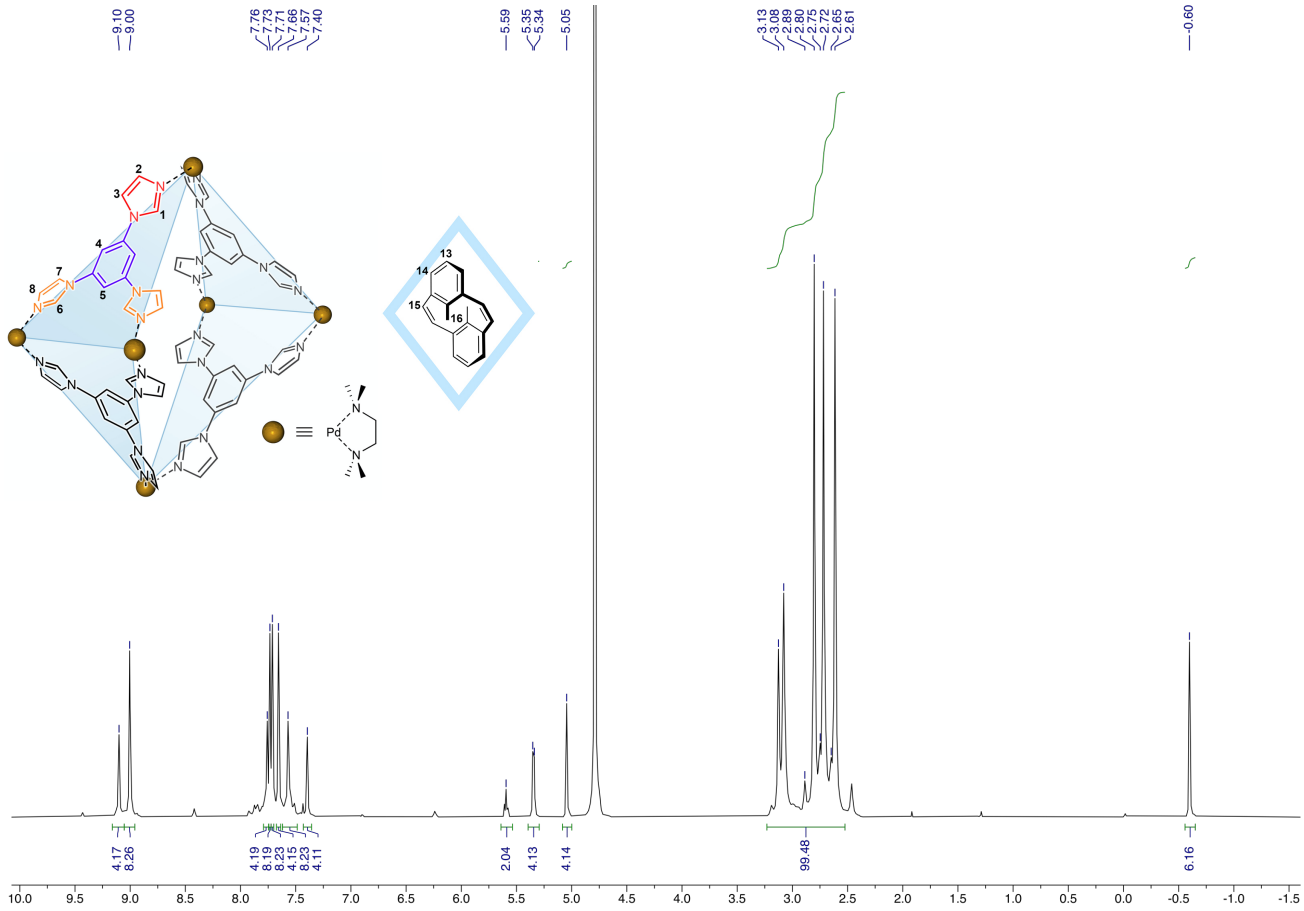


**Figure S17.** $^1$H NMR spectrum (500 MHz, $D_2O$) of CPD⊂**1**.

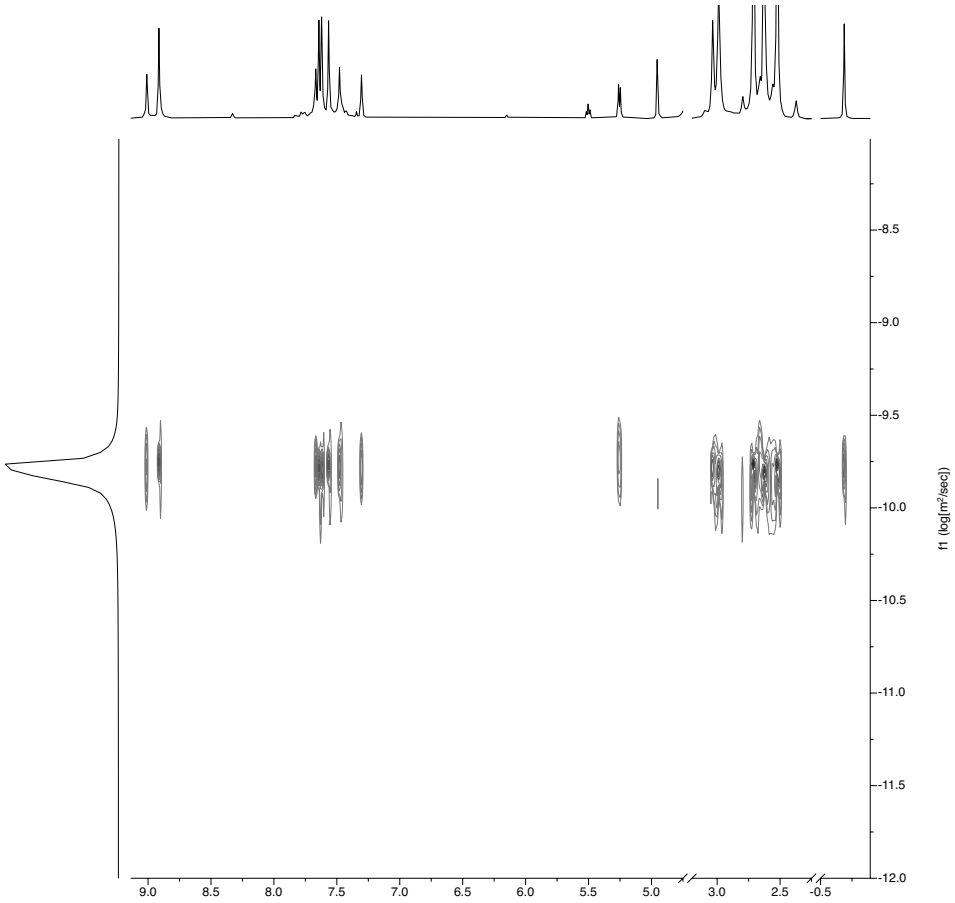


**Figure S18.** $^{1}$H DOSY NMR spectrum (500 MHz, $D_2O$) of CPD⊂**1**.

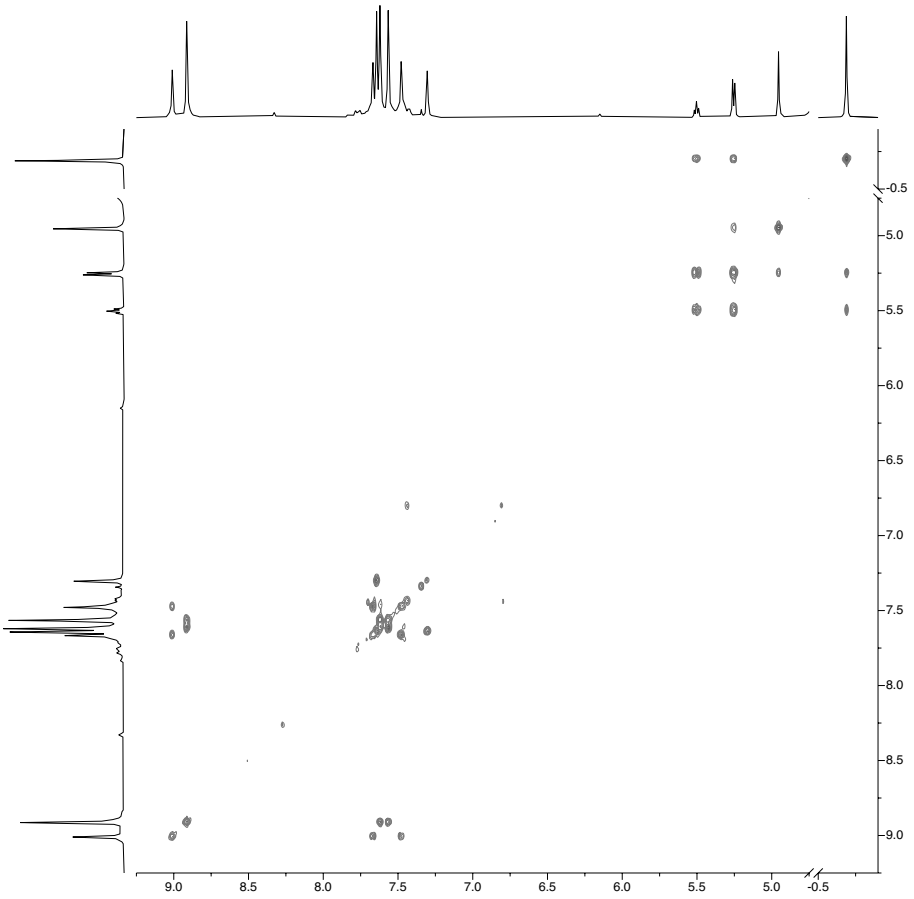


**Figure S19.** $^{1}H$–$^{1}H$ COSY NMR spectrum (500 MHz, $D_2O$) of CPD⊂**1**.

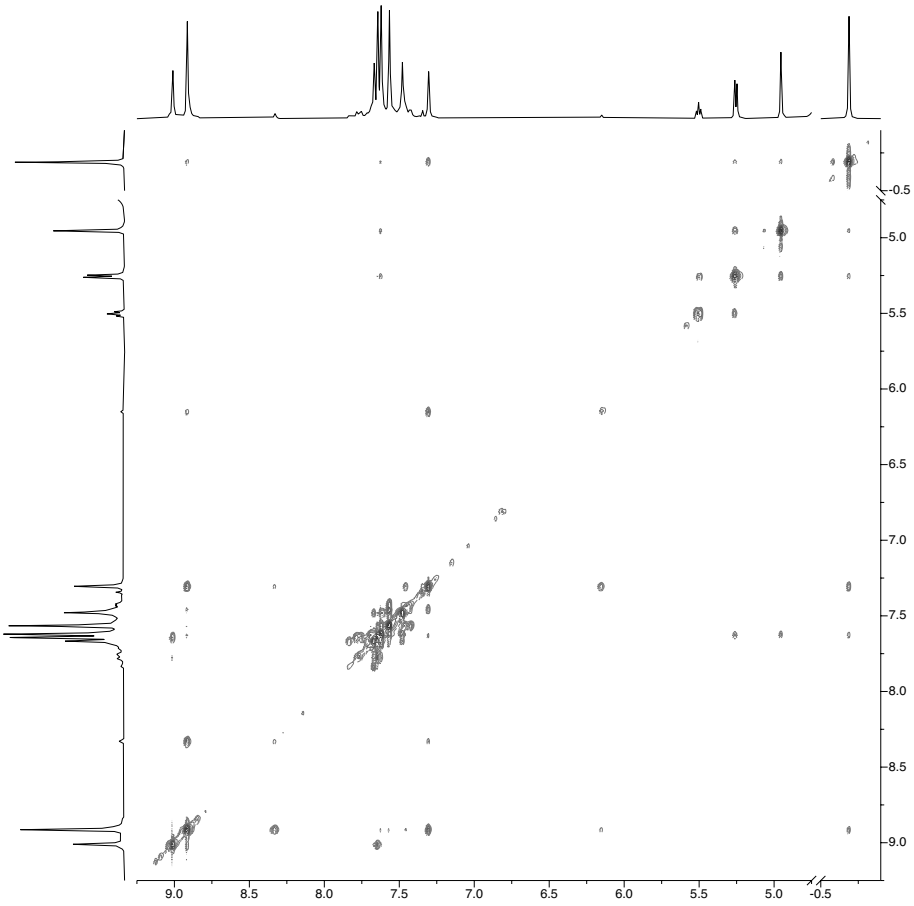


**Figure S20.** $^{1}$H–$^{1}$H NOESY NMR spectrum (500 MHz, $D_2O$) of CPD⊂**1**.

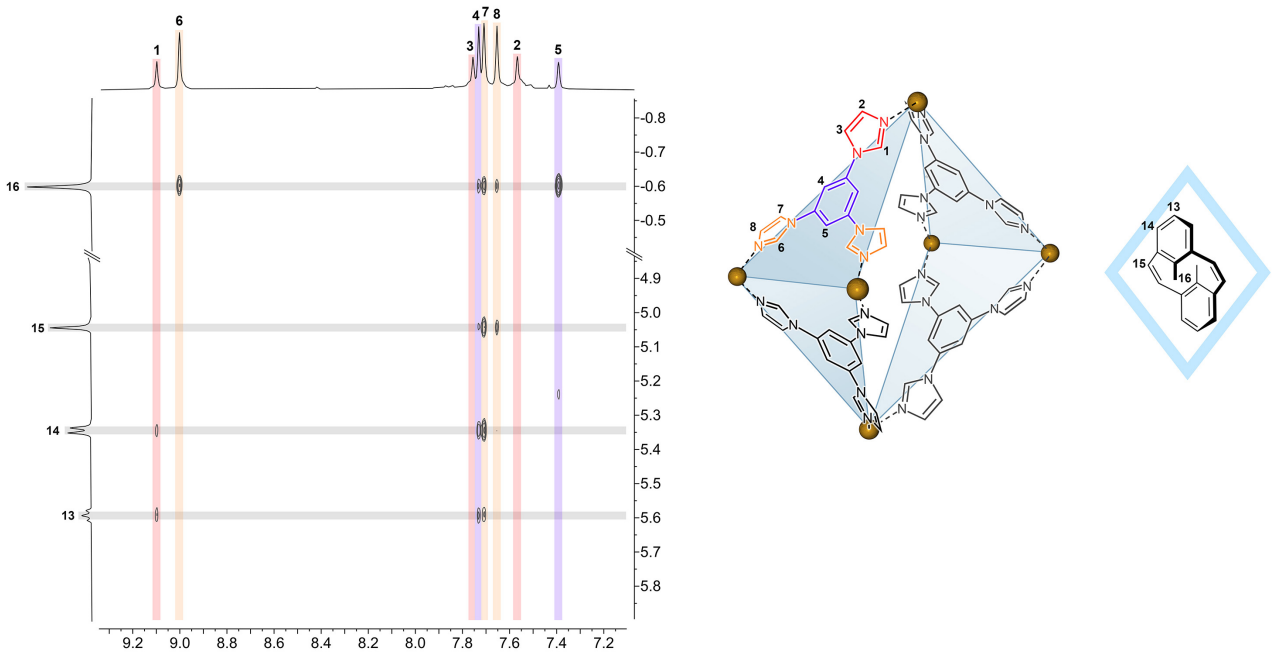


**Figure S21.** Partial $^{1}$H–$^{1}$H NOESY NMR spectrum (500 MHz, $D_2O$) of CPD⊂**1**.

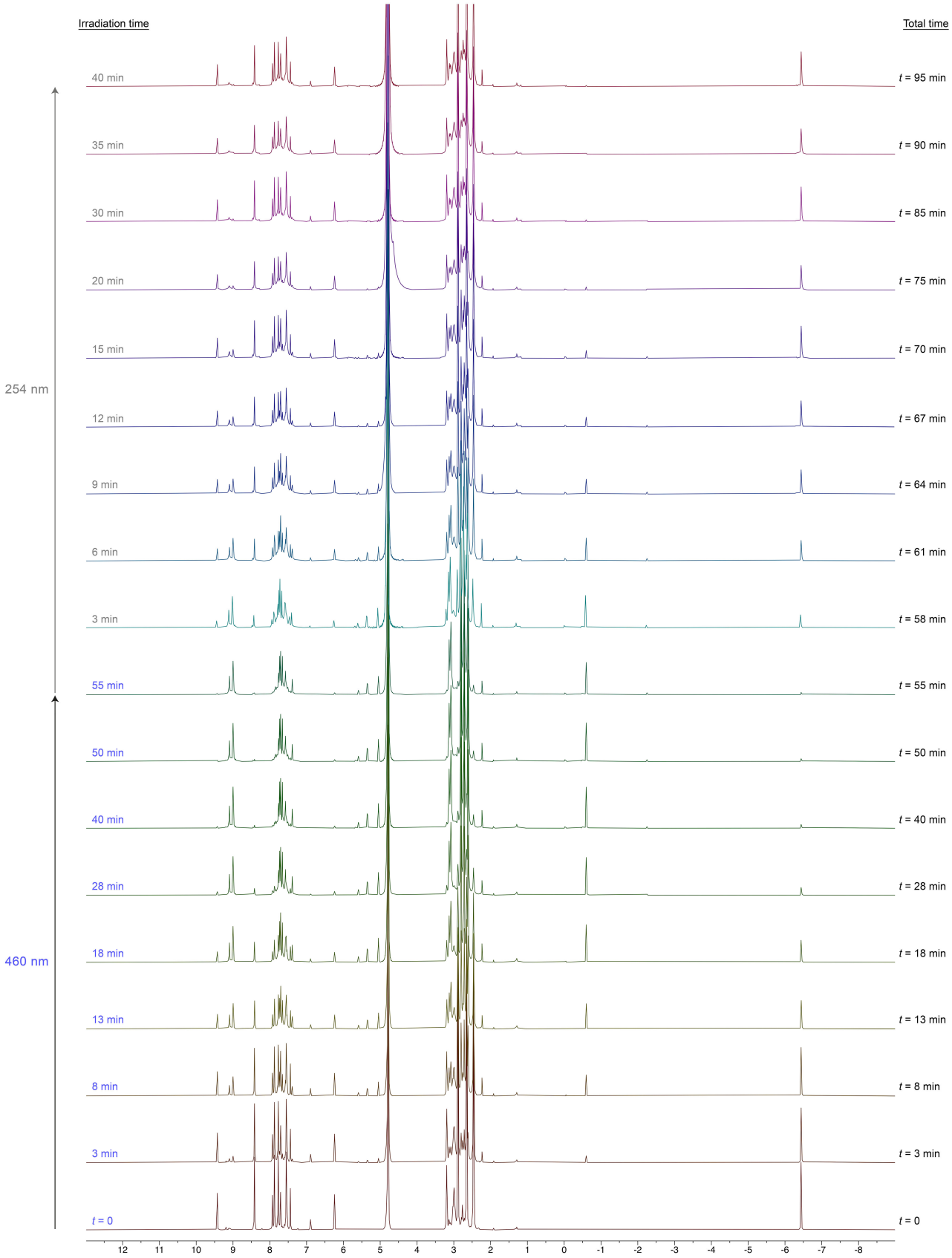


**Figure S22.** Full-range $^{1}$H NMR spectra (500 MHz, $D_2O$) of DHP⊂**1** before (bottom; $t$ = 0) and after different irradiation times with blue light, followed by UV light. Compositions of photostationary states derived from NMR: 6% DHP⊂**1** + 94% CPD⊂**1** under 460 nm light; 98% DHP⊂**1** + 2% CPD⊂**1** under 254 nm light.

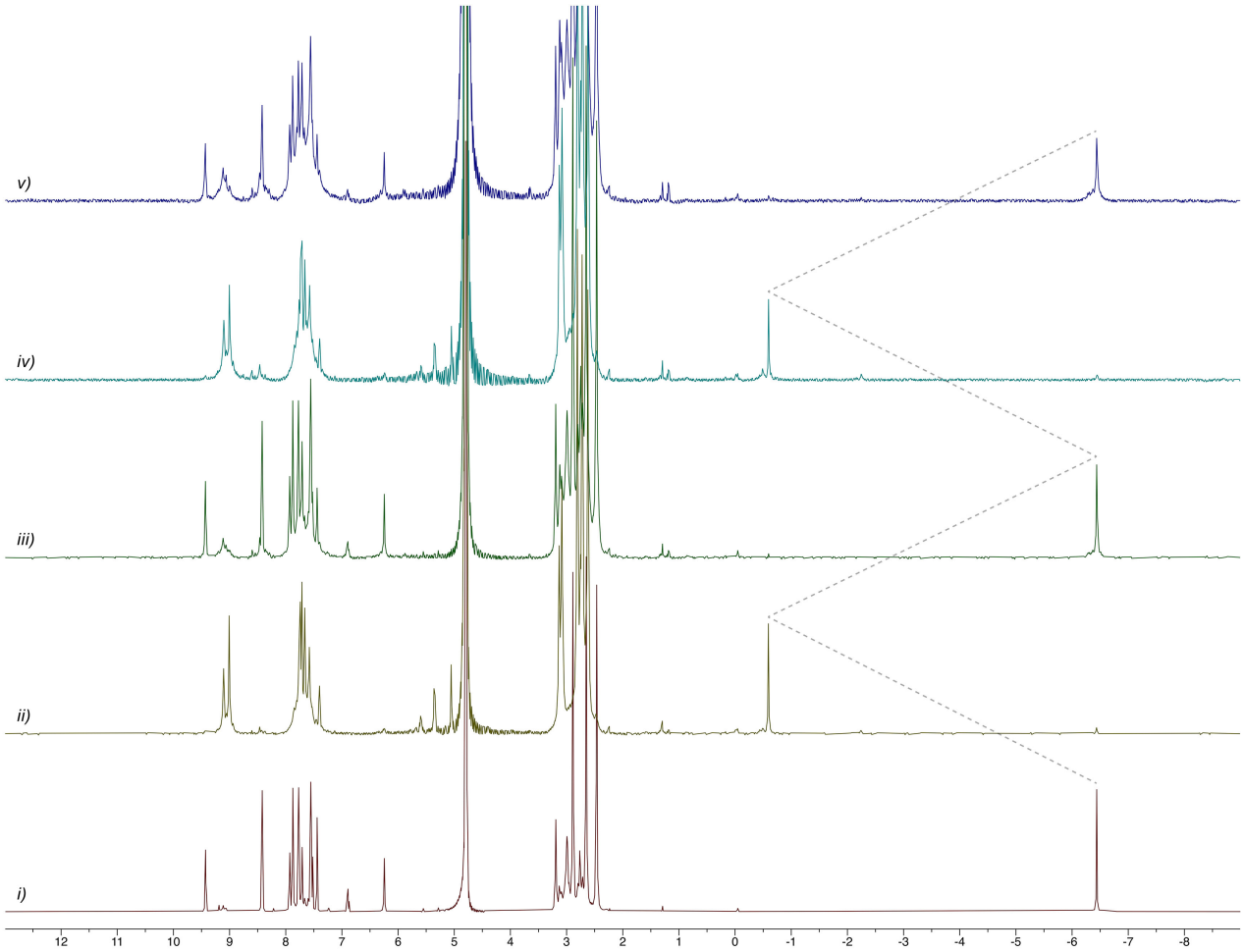


**Figure S23.** Two cycles of photoisomerization of DHP⊂**1** followed by $^{1}$H NMR spectroscopy (400 MHz, $D_2O$). From the bottom: *i)* initial spectrum before irradiation, *ii)* after 40 min of 460 nm, *iii)* after 30 min of 254 nm, *iv)* after 45 min of 460 nm, *v)* after 28 min of 254 nm.

## 11. Molecular dynamics simulations

Parametrization of the atomistic models

The atomistic model of cage **1** was taken from our recent work.[17] In particular, the cage model is parametrized according to the Generalized Amber Force Field.[17–19] DHP and CPD were parametrized consistently to **1**, via geometrical optimization and RESP calculation of the partial charges[20] performed using B3LYP functional[21] and the Pople 6-31G* basis set. These calculations were performed using Gaussian-16,[22] while the atomistic parametrization was carried out using the ANTECHAMBER software.[23]

Molecular dynamics simulations

All atomistic simulations in this work have been conducted using the GROMACS-2018.6 software[24] patched with PLUMED-2.[25] All systems were simulated for 1 μs of MD at the temperature of 297 K and pressure of 1 atm in explicit TIP3P water molecules[26] and in periodic boundary NPT conditions (constant N, number of particles, P, pressure, and T, temperature), employing the v-rescale thermostat[27] and the Berendsen barostat.[28] A timestep of 2 fs was used in the MD simulations. The electrostatic interactions were treated using particle mesh Ewald (PME).[29] The cutoff lengths of the real summation and of the VdW were set to 1.0 nm. The dynamics of the hydrogens was constrained using the LINCS algorithm.[30]

As recently done to model the encapsulation of azo compounds within cage **1**,[17] the starting conformations of DHP⊂**1** and CPD⊂**1** were obtained after a short MD run where the guests were encapsulated into the empty **1**, which was taken from the crystal structure of **1** containing two encapsulated azobenzene molecules[13] (CSD entry: TEZLAO20). The host–guest model systems were then equilibrated via MD simulations under the conditions described above. From the MD trajectories we then calculated the ensembles of configurations within 0.5 kcal/mol from the minimum energy configurations of the systems, which were then plotted (points and isolines in Figure 5a) on the FES of a native cage **1** taken from our previous work.[17] Representative snapshots of the minimum-free-energy configurations of DHP⊂**1** and CPD⊂**1** are shown in Figure S24 (corresponding to the cyan and green dots in the FES in Figure 5a).[28]

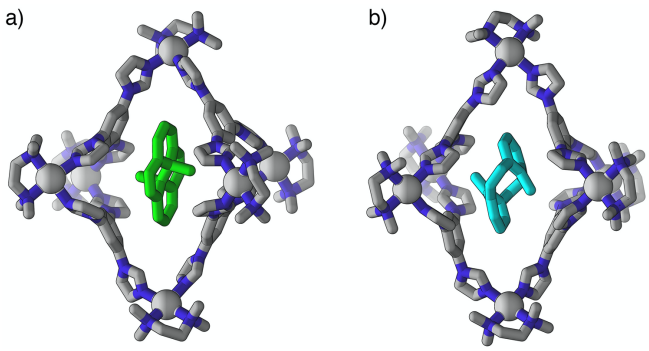


**Figure S24.** Representative $d_1/d_2$-minimum-free-energy configurations of DHP⊂**1** (a) and CPD⊂**1** (b).

## 12. Photoisomerization of free DHP in acetonitrile

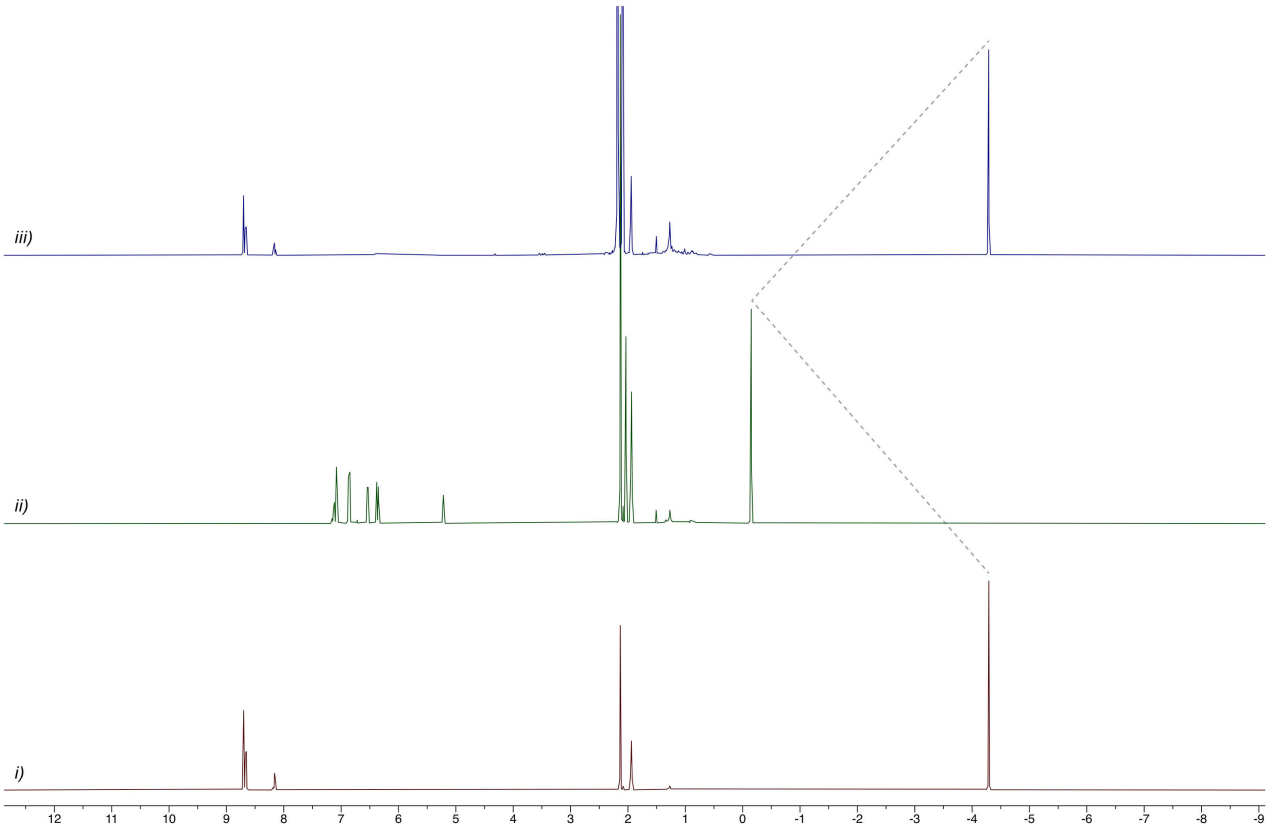


**Figure S25.** One cycle of photoisomerization of free DHP followed by $^{1}$H NMR spectroscopy (400 MHz, $CD_3CN$). From the bottom: *i)* initial spectrum before irradiation, *ii)* after 90 min of 460 nm, *iii)* after 90 min of 254 nm. The conversion is quantitative in both directions. Note, however, the appearance of decomposition products at ~1.5 ppm.

## 13. Photoisomerization of free DHP⊂**1** in non-deoxygenated water

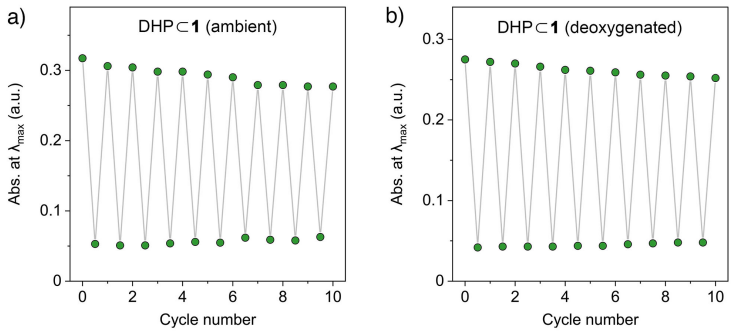


**Figure S26.** Reversible photoisomerization between DHP⊂**1** and CPD⊂**1** in non-deoxygenated water (a) and in deoxygenated water (b; replotted from Figure 7b in the main text) under otherwise identical conditions. In each cycle, the samples were exposed to 10 min of blue light ($\lambda$ = 460 nm) followed by 10 min of UV light ($\lambda$ = 254 nm). 13% and 8% decomposition over ten cycles was found over ten irradiation cycles in the presence and absence of oxygen, respectively.

## 14. Release of DHP from cage **1** upon addition of acetonitrile

150-µL aliquots of acetonitrile were added into an aqueous solution of DHP⊂**1** (1.5 mL, $1 \cdot 10^{-5}$ M) until a total volume of 3 mL was reached. After each addition, the solution was stirred and a UV/vis absorption spectrum was recorded. The data were corrected using a dilution factor which takes into account the ratio between the added volume of acetonitrile and the total volume present in the cuvette after each point, effectively normalizing the concentration of DHP in all spectra. The resulting plot shows an increase in the absorbance of DHP as acetonitrile is added to the solution. Free DHP has a higher absorption coefficient in the UV region compared to encapsulated DHP; these results therefore suggest that DHP is released from cage **1** upon addition of acetonitrile. Furthermore, the absorption maximum for DHP shifts from 346 nm (characteristic of DHP⊂**1**) to 336 nm (characteristic of free DHP in acetonitrile). No precipitation was observed over the course of this experiment.

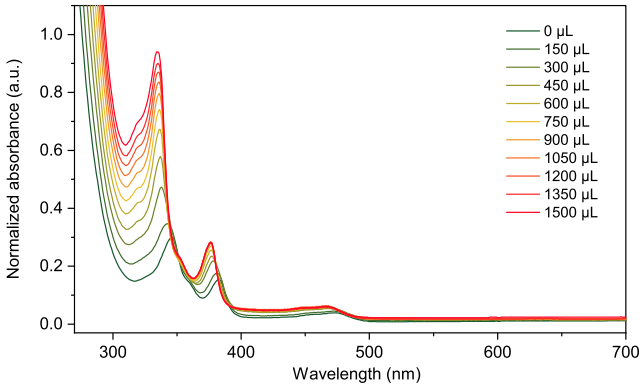


**Figure S27.** Normalized UV/vis absorption spectra following sequential additional of acetonitrile to an aqueous solution of DHP⊂**1**.

## 15. Supplementary references


1. Fan, J.; Gan, L.; Kawaguchi, H.; Sun, W.-Y.; Yu, K.-B.; Tang, W.-X. Reversible Anion Exchanges between the Layered Organic–Inorganic Hybridized Architectures: Syntheses and Structures of Manganese(II) and Copper(II) Complexes Containing Novel Tripodal Ligands. *Chem. - Eur. J.* **2003**, *9*, 3965–3973.
2. Samanta, D.; Mukherjee, S.; Patil, Y. P.; Mukherjee, P. S. Self-Assembled $Pd_6$ Open Cage with Triimidazole Walls and the Use of Its Confined Nanospace for Catalytic Knoevenagel- and Diels–Alder Reactions in Aqueous Medium. *Chem. - Eur. J.* **2012**, *18*, 12322–12329.
3. Mitchell, R. H.; Boekelheide, V. Transformation of Sulfide Linkages to Carbon–Carbon Double Bonds. Syntheses of *cis*- and *trans*-15,16-Dimethyldihydropyrene and *trans*-15,16-Dihydropyrene. *J. Am. Chem. Soc*. **1974**, *96*, 1547–1557.
4. Mitchell, R. H.; Carruthers, R. J.; Mazuch, L.; Dingle T. W. Toward the Understanding of Benzannelated Annulenes: Synthesis and Properties of [*a*]-Ring Monobenzannelated Dihydropyrenes. *J. Am. Chem. Soc.* **1982**, *104*, 2544–2551.
5. Lindsay, W. S.; Stokes, P.; Humber, L. G.; Boekelheide, V. Syntheses of 4,12-Dimethyl[2.2]metacyclophane. *J. Am. Chem. Soc.* **1961**, *83*, 943–949.
6. Williams, R. V.; Armantrout, J. R.; Twamley, B.; Mitchell, R. H.; Ward, T. R.; Bandyopadhyay, S. A. Theoretical and Experimental Scale of Aromaticity. The First Nucleus-Independent Chemical Shifts (NICS) Study of the Dimethyldihydropyrene Nucleus. *J. Am. Chem. Soc*. **2002**, *124*, 13495–13505.
7. Sheldrick, G. M. *SHELXT* – Integrated space-group and crystal structure determination. *Acta Crystallogr. Sect. A* **2015**, *71*, 3–8.
8. Sheldrick, G. M. Crystal structure refinement with *SHELXL*. *Acta Crystallogr. Sect. C* **2015**, *71*, 3–8.

9. Dolomanov, O. V.; Bourhis, L. J.; Gildea, R. J.; Howard, J. A. K.; Puschmann, H. *OLEX2*: a complete structure solution, refinement and analysis program. *J. Appl. Crystallogr.* **2009**, *42*, 339–341.
10. Spek, A. L. PLATON SQUEEZE: a tool for the calculation of the disordered solvent contribution to the calculated structure factors. *Acta Crystallogr. Sect. C* **2015**, *71*, 9–18.
11. Samanta, D.; Galaktionova, D.; Gemen, J.; Shimon, L. J. W.; Diskin-Posner, Y.; Avram, L.; Král, P.; Klajn, R. Reversible chromism of spiropyran in the cavity of a flexible coordination cage. *Nat. Commun.* **2018**, *9*, 641.
12. Hanopolskyi, A. I.; De, S.; Białek, M. J.; Diskin-Posner, Y.; Avram, L.; Feller, M.; Klajn, R. Reversible switching of arylazopyrazole within a metal–organic cage. *Beilstein J. Org. Chem.* **2019**, *15*, 2398–2407.
13. Samanta, D.; Gemen, J.; Chu, Z.; Diskin-Posner, Y.; Shimon, L. J. W.; Klajn, R. Reversible photoswitching of encapsulated azobenzenes in water, *Proc. Natl. Acad. Sci. USA* **2018**, *115*, 9379–9384.
14. Williams, R. V.; Edwards, W. D.; Vij, A.; Tolbert, R. W. Theoretical Study and X-ray Structure Determination of Dimethyldihydropyrene. *J. Org. Chem.* **1998**, *63*, 3125–3127.
15. Shi, Z.; Peng, P.; Strohecker, D.; Liao, Y. Long-Lived Photoacid Based upon a Photochromic Reaction. *J. Am. Chem. Soc.* **2011**, *133*, 14699–14703.
16. Stafforst, T.; Hilvert, D. Kinetic characterization of spiropyrans in aqueous media. *Chem. Commun*. **2009**, 287–288.
17. Pesce, L.; Perego, C.; Grommet, A. B.; Klajn, R.; Pavan, G. M. Molecular Factors Controlling the Isomerization of Azobenzenes in the Cavity of a Flexible Coordination Cage. *J. Am. Chem. Soc.* **2020**, 142, 9792–9802.
18. Wang, J.; Wolf, R. M.; Caldwell, J. W.; Kollman, P. A.; Case, D. A. Development and Testing of a General Amber Force Field. *J. Comput. Chem.* **2004**, *25*, 1157–1174.
19. Li, P.; Merz, K. M. MCPB.py: A Python Based Metal Center Parameter Builder. *J. Chem. Inf. Model.* **2016**, *56*, 599–604.
20. Bayly, C. I.; Cieplak, P.; Cornell, W.; Kollman, P. A. A Well-Behaved Electrostatic Potential Based Method Using Charge Restraints for Deriving Atomic Charges: The RESP Model. *J. Phys. Chem.* **1993**, *97*, 10269–10280.
21. Becke, A. D. Density-Functional Thermochemistry. III. The Role of Exact Exchange. *J. Chem. Phys.* **1993**, *98*, 5648–5652.
22. Frisch, M. J.; Trucks, G. W.; Schlegel, H. B.; Scuseria, G. E.; Robb, M. A.; Cheeseman, J. R.; Montgomery; Jr.; J. A.; Vreven, T.; et al. *Gaussian 03*; Gaussian, Inc.: Wallingford, CT, **2004**.
23. Wang, J.; Wang, W.; Kollman, P.; Case, D. Antechamber, An Accessory Software Package For Molecular Mechanical Calculations. Submitted to *J. Chem. Inf. Comp. Sci.* **2000**.
24. Hess, B.; Kutzner, C.; van der Spoel, D.; Lindahl, E. GROMACS 4: Algorithms for Highly Efficient, Load-Balanced, and Scalable Molecular Simulation. *J. Chem. Theory Comput.* **2008**, *4*, 435–447.
25. Tribello, G. A.; Bonomi, M.; Branduardi, D.; Camilloni, C.; Bussi, G. PLUMED 2: New feathers for an old bird. *Comput. Phys. Commun.* **2014**, *185*, 604–613.
26. Jorgensen, W. L.; Chandrasekhar, J.; Madura, J. D.; Impey, R. W.; Klein, M. L. Comparison of Simple Potential Functions for Simulating Liquid Water. *J. Chem. Phys.* **1983**, *79*, 926–935.
27. Bussi, G.; Donadio, D.; Parrinello, M. Canonical Sampling through Velocity Rescaling. *J. Chem. Phys.* **2007**, *126*, 014101.
28. Berendsen, H. J. C.; Postma, J. P. M.; van Gunsteren, W. F.; DiNola, A.; Haak, J. R. Molecular dynamics with coupling to an external bath. *J. Chem. Phys.* **1984**, *81*, 3684–3690.
29. Essmann, U.; Perera, L.; Berkowitz, M. L.; Darden, T.; Lee, H.; Pedersen, L. G. A smooth particle mesh Ewald method. *J. Chem. Phys.* **1995**, *103*, 8577–8593.
30. Hess, B.; Bekker, H.; Berendsen, H.; Fraaije, J. LINCS: A linear constraint solver for molecular simulations. *J. Comput. Chem.* **1998**, *18*, 1463–1472.